Acta Mechanica Sinica (2019) 35(1):70–77
https://doi.org/10.1007/s10409-018-0800-1

RESEARCH PAPER

Dual-level stress plateaus in honeycombs subjected to impact loading: perspectives from bucklewaves, buckling and cell-wall progressive folding

Lang Li[1,2,3] · Zhenyu Zhao[1,3] · Rui Zhang[1,3] · Bin Han[4,5,6] · Qiancheng Zhang[1,3] · Tian Jian Lu[2,3]

Received: 4 April 2018 / Revised: 29 May 2018 / Accepted: 4 July 2018 / Published online: 20 September 2018

Abstract
Dual-level stress plateaus (i.e., relatively short peak stress plateaus, followed by prolonged crushing stress plateaus) in metallic hexagonal honeycombs subjected to out-of-plane impact loading are characterized using a combined numerical and analytical study, with the influence of the strain-rate sensitivity of the honeycomb parent material accounted for. The predictions are validated against existing experimental measurements, and good agreement is achieved. It is demonstrated that honeycombs exhibit dual-level stress plateaus when bucklewaves are initiated and propagate in cell walls, followed by buckling and progressive folding of the cell walls. The abrupt stress drop from peak to crushing plateau in the compressive stress versus strain curve can be explained in a way similar to the quasi-static buckling of a clamped plate. The duration of the peak stress plateau is more evident for strain-rate insensitive honeycombs.

Keywords Honeycomb · Impact loading · Dual-level stress · Strain-rate sensitivity

1 Introduction

When metallic honeycombs are designed as lightweight impact energy absorbers to withstand impulse loading, it is important to characterize their dynamical compressive behaviors and explore the physical mechanisms underlying such behaviors. Although numerous efforts have been devoted to studying the out-of-plane compression of metallic honeycombs [1–10], most focused on quasi-static loading and low-speed impact cases. The dynamic compressive behaviors of honeycombs subjected to intense out-of-plane impulse loading remain elusive, especially from analytical and numerical points of view.

The fundamental mechanisms underlying the out-of-plane compression performance of aluminum hexagonal honeycombs subjected to quasi-static loading are well understood [1–5]. Typically, the quasi-static stress versus strain curve starts with an elastic regime where the response is initially stiff and nearly linear, then becomes nonlinear elastic due to elastic buckling of cell walls. At higher stress levels, the elastic regime ends with a peak stress and the honeycomb starts to collapse, with stress softening due to cell wall bending and formation of localized plastic hinges. Followed by the onset of collapse, the cell walls are progressively folded, causing an apparent stress plateau regime in the stress versus strain curve. Finally, the stress plateau regime is terminated by densified folds and the stress increases rapidly beyond the densification strain.

✉ Bin Han
hanbinghost@mail.xjtu.edu.cn

✉ Tian Jian Lu
tjlu@mail.xjtu.edu.cn

1 State Key Laboratory for Strength and Vibration of Mechanical Structures, Xi'an Jiaotong University, Xi'an 710049, China

2 State Key Laboratory of Mechanics and Control of Mechanical Structures, Nanjing University of Aeronautics and Astronautics, Nanjing 210016, China

3 MOE Key Laboratory for Multifunctional Materials and Structures, Xi'an Jiaotong University, Xi'an 710049, China

4 School of Mechanical Engineering, Xi'an Jiaotong University, Xi'an 710049, China

5 School of Engineering, Brown University, Providence, RI 02912, USA

6 Research Institute of Xi'an Jiaotong University, Zhejiang, Hangzhou 311215, China

When subjected to low-speed impact, the response is similar to that under quasi-static loading, except for obvious strength enhancement in both the peak stress and crushing stress plateau regimes [6–10]. This enhancement has been attributed to the strain-rate sensitivity of the parent material as well as to the dynamic inertial stabilization of cell walls against buckling. While strain-rate sensitivity enhances both the peak and crushing stresses by elevating the flow stress of the parent material, inertial stabilization enhances the buckling strength due to the activation of higher order buckling modes (or smaller wavelengths) [11].

When subjected to high-speed impact loading, the out-of-plane compressive response of a honeycomb can be quite different from that under either quasi-static or low-speed impact loading. For instance, based on experimental observations, Harrigan et al. [12] identified dual-level stress plateaus for hexagonal honeycombs subjected to high-speed impact loading, namely, the peak stress plateau which is relatively short, and the crushing stress plateau which is much prolonged. Similar phenomena were observed in prismatic sandwich cores (e.g., I, X, and Y-cores) and square honeycombs under high-speed impact loading [13–16]. Interestingly, however, the prismatic cores and square honeycombs exhibit significantly prolonged duration of peak stress plateau relative to the hexagonal honeycombs. Although it is believed that the peak stress plateau is a result of plastic wave propagation [17–19], the critical event triggering the remarkable stress drop from the peak plateau to the crushing plateau still needs further investigation. Further, analytical models capable of predicting the dual-level stress plateaus, especially when strain-rate sensitivity is considered, are still lacking.

The current study aims to explore the physical mechanisms that govern the appearance of dual-level stress plateaus in metallic hexagonal honeycombs subjected to out-of-plane high-speed impact loading. Since it is, at present, difficult to experimentally observe and quantify plastic wave propagation in cell walls, which is of significant importance for understanding the dual-level stress plateaus phenomenon, a combined numerical and analytical study is carried out. A finite element (FE) model for hexagonal honeycombs subjected to out-of-plane impact loading is constructed, which is validated by comparing simulation results with existing experimental data. Systematic FE simulations are then performed by varying the impact velocity from 30 m/s to 170 m/s, with the physical mechanisms underlying the corresponding compressive responses explored. Built upon the mechanisms identified, an analytical model is developed with the strain-rate sensitivity of the parent material accounted for.

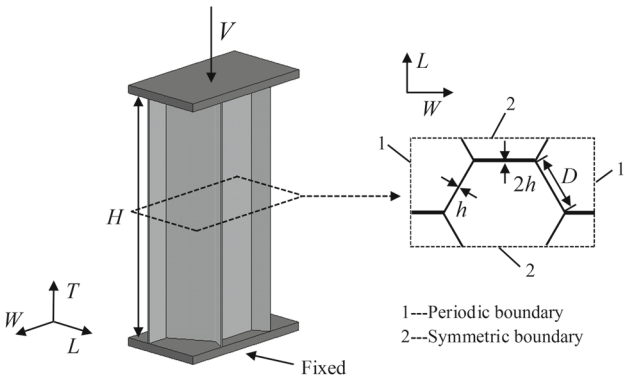

Fig. 1 Schematic of periodic FE model for hexagonal honeycomb

2 FE simulation

2.1 FE model

Numerical simulation models of hexagonal aluminum honeycombs are constructed using the commercially available FE code ANSYS/LS-DYNA. Due to periodicity and symmetry, only one unit cell in the L direction with symmetric boundaries in the W direction is considered, as shown in Fig. 1. For the case considered here, the honeycomb block with cell wall length D and cell wall thicknesses h and $2h$ for single-thickness walls and double-thickness walls, respectively, is sandwiched between two rigid plates. The height of the honeycomb block is H. The supporting plate is fixed, while the impact plate moves downwards to compress the honeycomb with a prescribed constant velocity V. Unless otherwise stated, $D = 3$ mm, $h = 0.05$ mm, and $H = 15$ mm are selected.

Cell walls are discretized using solid elements (solid164), with at least three elements placed across the cell wall thickness. Mesh sensitivity study shows that an element size of 0.05 mm is sufficient to achieve numerical convergence. Single surface contact is employed on cell walls, and automatic node-to-surface contact is applied between the honeycomb block and the rigid plates. A friction coefficient of 0.15 is adopted for all contact interactions [20].

With strain-rate and strain hardening effects taken into account, a bi-linear constitutive relation is adopted for cell wall material, as

$$\sigma = \begin{cases} E_s \varepsilon, & \varepsilon \le \frac{\sigma_y^s}{E_s}, \\ \sigma_y^s + E_t\left(\varepsilon - \frac{\sigma_y^s}{E_s}\right), & \varepsilon > \frac{\sigma_y^s}{E_s}, \end{cases} \tag{1}$$

where $\sigma_y^s = \sigma_{ys}$ is the static flow stress, which is replaced by the dynamic flow stress σ_y^d when strain-rate sensitivity of

Table 1 Mechanical properties of the parent material for aluminum honeycombs

E (GPa)	σ_{ys} (MPa)	ρ_s (kg/m^3)	E_t (MPa)	ν	C (s^{-1})	P
69	126.8	2700	278.7	0.33	6500	4

cell wall material is considered. To this end, the well-known Cowper–Symonds relation is employed

$$\sigma_y^d = \sigma_y^s \left[1 + \left(\frac{\dot{\varepsilon}}{C} \right)^{1/P} \right], \tag{2}$$

where $\dot{\varepsilon}$ denotes the strain-rate, and C and P are the strain-rate parameters [21]. The parent material of the honeycomb is selected as aluminum (Al3003-H24) [22, 23]. Its mechanical properties are listed in Table 1.

2.2 Validation of FE model

To validate the FE model, the numerical simulation results are compared with existing experimental measurements [12]. For the validation, the geometry of the FE model is constructed in accordance with the honeycomb specimen used in Ref. [12], and the same parent material is selected. As shown in Fig. 2, with the impact velocity fixed at 128 m/s, the present FE simulations not only reproduce the dual-level stress plateaus observed experimentally, but also show reasonable agreement with the experimentally measured peak plateau stress (σ^d_{peak}), crushing plateau stress ($\sigma^d_{plateau}$) and truncation strain (ε_t). The truncation strain refers to the instant when the peak plateau ends. In the current study, for simplicity, it is assumed that it may be defined as the strain when the stress drops to 95% of the average value of the stress ahead of the strain. It should be mentioned that the original experimental data [12] exhibited a delayed elastic regime, which has been ignored in Fig. 2 so as to show more clearly the stress plateaus.

3 Dynamic compressive response of honeycombs

The FE model, as validated above, is now employed to calculate the stress versus strain curves exerted on the impact face of the present hexagonal aluminum honeycombs, as shown in Fig. 3a, b for both strain-rate insensitive and sensitive honeycombs, respectively, with $h/D = 0.167$. Strain-rate sensitivity is seen to elevate both plateaus but reduce the duration of the peak plateau. To have a comprehensive understanding of the underlying mechanisms, strain-rate

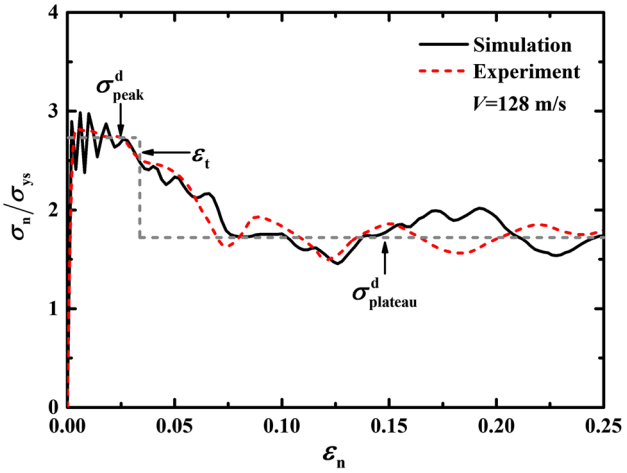

Fig. 2 FE simulation results compared with existing experimental measurements for out-of-plane compression of hexagonal aluminum honeycomb at impact velocity of 128 m/s [12]

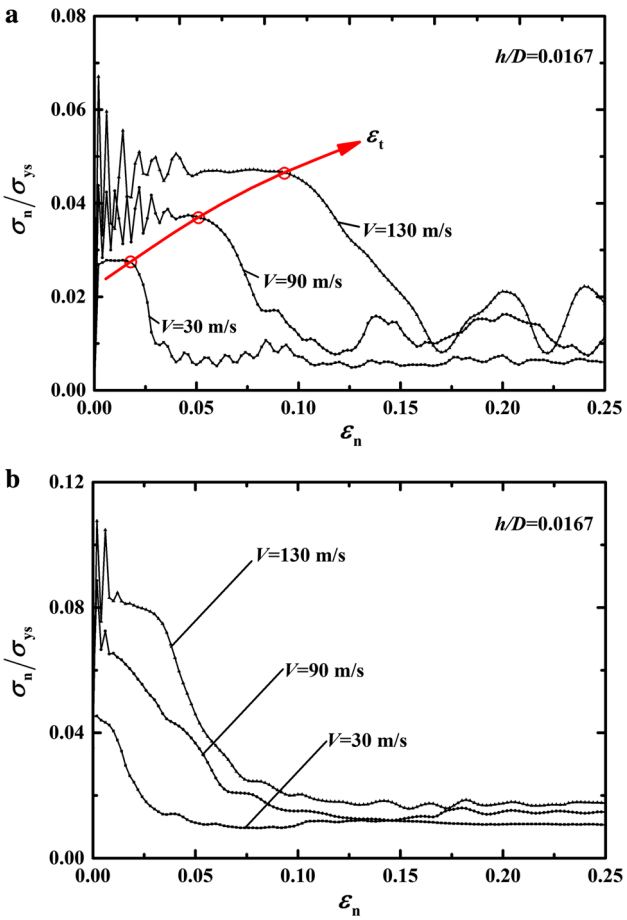

Fig. 3 Out-of-plane compressive stress versus strain curves of honeycomb made from **a** strain-rate insensitive and **b** strain-rate sensitive parent material under selected impact velocities

insensitive honeycombs are investigated in this section; the effect of strain-rate sensitivity will be discussed in the next section.

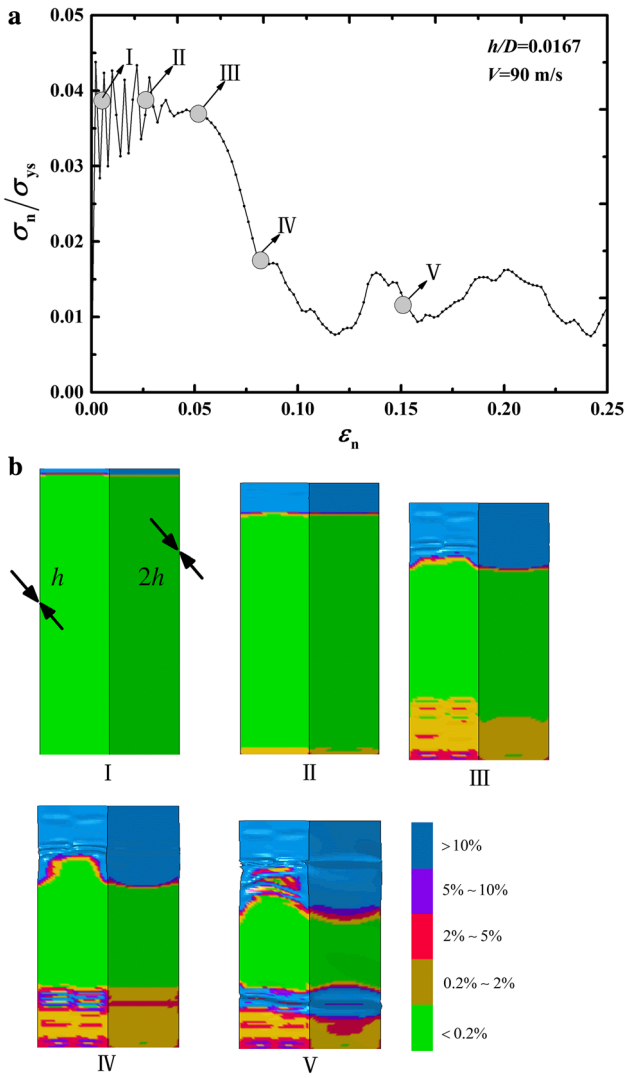

Fig. 4 **a** Stress versus strain curve at impact velocity of 90 m/s and **b** contours of plastic strain corresponding to each point marked in plot **a**

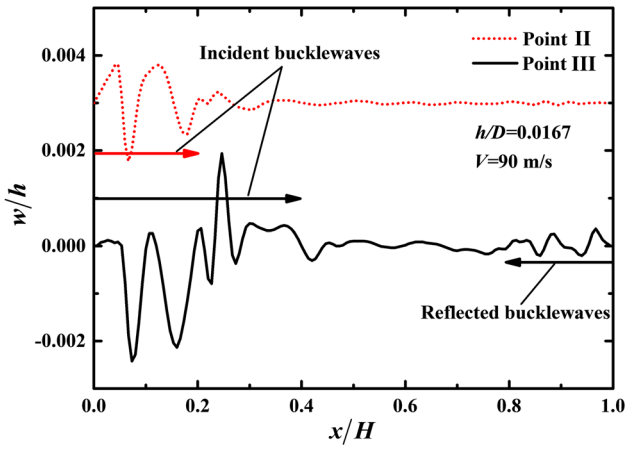

Fig. 5 Buckle patterns of single thickness (h) cell wall (Fig. 4b) along the Lagrange location of cell wall height, with w/h denoting normalized transverse deflection of cell wall

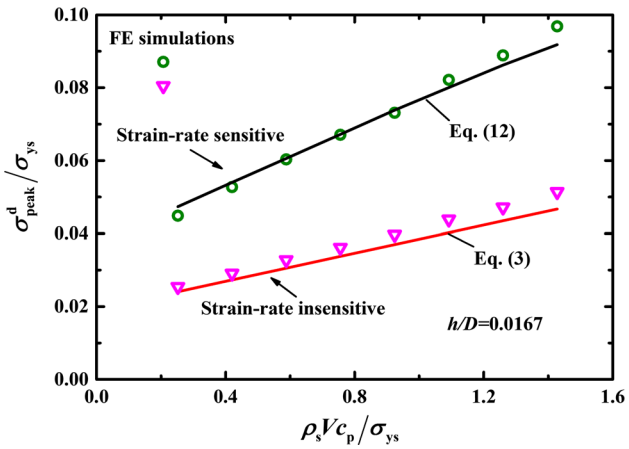

Fig. 6 Theoretically predicted peak plateau stress compared with FE simulations over a wide range of the dimensionless loading index $\rho_s V c_p/\sigma_{ys}$

As is shown in Fig. 3a, the peak stress, crushing stress and truncation strain all increase with increasing impact velocity. For further insight, the evolution of plastic strain contours for a corner element adjoining single and double thickness cell walls of the hexagonal honeycomb are plotted in Fig. 4. The dynamic compressive response of the honeycomb is seen to be a successive process including bucklewave propagation in cell walls, buckling and progressive folding of cell walls, as illustrated in more detail immediately below.

3.1 Propagation of bucklewaves in cell walls

With reference to Fig. 4, upon impact loading, an incident plastic wave front with large plastic strain (>10%) initiates at the impact side and propagates towards the fixed end of the honeycomb (point I). Then, an opposing plastic wave front with small plastic strain (within the range of 0.2%–2%) forms at the fixed end due to reflection of the elastic wave (point II). During this stage, the stress remains at the peak plateau level until a critical event is reached that triggers the stress drop at point III, while additional evidence (Fig. 5) indicates that short wave buckles are coupled with the propagation of the plastic wave front. Due to dynamic inertial stabilization, the short wave buckles do not induce cell wall buckling, suggesting that the peak stress plateau is a result of the propagation of bucklewaves. Prior to the onset of cell wall buckling, classical one-dimensional (1D) elastic–plastic wave theory can be employed to calculate the peak stress of hexagonal honeycombs (with strain-rate sensitivity ignored), as

$$\sigma_{\text{peak}}^{\text{d}} = \sigma_{\text{ys}}\overline{\rho} + \rho_{\text{c}} V c_{\text{p}} = \sigma_{\text{ys}}\overline{\rho}\left(1 + \frac{\rho_{\text{s}} V c_{\text{p}}}{\sigma_{\text{ys}}}\right), \tag{3}$$

where $c_p \equiv \sqrt{E_t/\rho_s}$ is the plastic wave speed, $\rho_c \equiv \overline{\rho}\rho_s$ is the density of honeycomb, and $\overline{\rho}$ is the relative density of honeycomb. Figure 6 compares the theoretical prediction of Eq. (3) with the FE calculation. Relatively good agreement is achieved, and it is seen that the (normalized) peak stress is linearly proportional to the dimensionless loading index $\rho_s V c_p/\sigma_{ys}$.

3.2 Buckling of cell walls

As shown in Fig. 4a, the stress drops rapidly from point III to IV. Correspondingly, the plastic strain contours of Fig. 4b reveal that bucklewaves stop propagating in the single-thickness cell wall while obvious buckling is observed behind the incident plastic wave front. In contrast, in the cell wall of double thickness, the plastic wave front is still propagating, with no obvious buckling observed. These phenomena indicate that, upon reaching the crushing stress plateau, the rapid stress drop from III to IV is caused by buckling of single-thickness cell walls. Beyond point IV, obvious buckling is also observed in double-thickness cell walls and the stress continues to drop until reaching the crushing plateau (Fig. 4b: point V). Thus, buckling is dependent on cell wall thickness, and a thicker cell wall can sustain a larger strain without buckling. These findings are different from those of prismatic cores, wherein stress drop occurs when the incident plastic wave arrives at the fixed end [13–16].

To estimate the duration of the peak plateau, denoted here by the truncation strain ε_t (Figs. 2 and 3), the physical state of the plastic region behind the wave front for single-thickness cell walls is analyzed. This plastic region is in a state of uniform stress $\sigma_{ys}\left(1+\rho_s V c_p/\sigma_{ys}\right)$, constant particle velocity V and constant plastic strain V/c_p so that, to a good approximation, it may be treated as a quasi-static region. As a result, the onset of quasi-static buckling of a clamped plate may be taken as the critical event triggering the stress drop, as the wave front may be treated as a clamped end [17]. Under such conditions, the critical length L_c of the plastic region prior to buckling can be analytically calculated, as

$$L_c = \pi h\sqrt{\frac{E_t}{3\sigma_{ys}\left(1+\rho_s V c_p/\sigma_{ys}\right)}}. \tag{4}$$

It follows that the strain ε_t at which the propagation of bucklewaves is truncated by the buckling of single-thickness cell walls is given by

$$\varepsilon_t = \frac{V/c_p}{1-V/c_p}\cdot\frac{L_c}{H}. \tag{5}$$

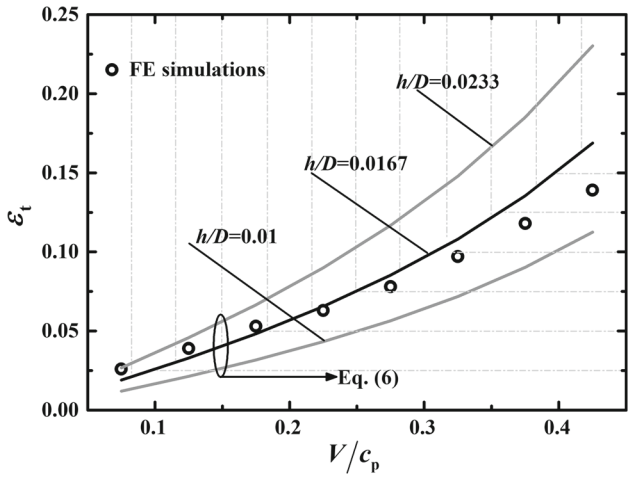

Fig. 7 Truncation strain plotted as a function of impact velocity: Analytical predictions compared with FE simulations

Combining Eqs. (3–5) yields

$$\varepsilon_t = \pi\frac{V/c_p}{1-V/c_p}\cdot\frac{h}{H}\left[\frac{3\sigma_{ys}}{E_t}\left(1+\frac{\rho_s V c_p}{\sigma_{ys}}\right)\right]^{-1/2}. \tag{6}$$

By comparing the truncation strain predicted by Eq. (6) with FE simulation (Fig. 7), the assumption of quasi-static buckling is seen to be reasonable in explaining the stress drop phenomenon. Further, the results of Fig. 7 demonstrate that the truncation strain increases with increasing impact velocity or increasing cell wall aspect ratio h/D. Inspection of Eq. (6) reveals that increasing the impact velocity increases the truncation strain via the coefficient $\frac{V/c_p}{1-V/c_p}$, while increasing the cell wall aspect ratio enhances stabilization of cell walls against buckling (thus leading to a larger truncation strain). These findings also explain why the prismatic cores and square honeycombs exhibit significantly prolonged duration of peak stress plateaus relative to hexagonal honeycombs, because the former have much larger cell wall aspect ratios and much higher strain hardening parent materials than the latter.

3.3 Progressive folding of cell walls

Once buckling occurs in a cell wall having either single or double thickness, the cell wall starts to fold progressively, which defines a dynamic crushing plateau stress $\sigma^d_{plateau}$ at the impact side. This dynamic crushing plateau stress cannot be predicted by shock theory, as is done in Ref. [24], because the assumption of particle velocity discontinuity related to stress discontinuity at the shock wave front can no longer hold when analyzing structures with local structural softening, such as honeycombs under out-of-plane loading [25, 26].

An alternative approach detailed in Ref. [26] is employed, as illustrated below.

The phenomenological model in Ref. [26] assumes that the formation of the second fold begins after the first fold has completely collapsed and the material of the second fold begins to support loading. Therefore, the dynamic mean supporting force per unit area during folding is governed by the dynamic collapse stress of the wall material, given as

$$\sigma_0^{\mathrm{d}} = \sigma_0\left(1 + \frac{\rho_{\mathrm{s}} V c_{\mathrm{p}}}{\sigma_{\mathrm{ys}}}\right), \tag{7}$$

where σ_0 denotes the quasi-static plateau stress, given by [1]

$$\sigma_0 = 6.63\sigma_{\mathrm{ys}}\left(\frac{h}{D}\right)^{5/3}. \tag{8}$$

During folding, the fold is accelerated from still to speed V. Conservation of momentum then dictates that

$$\left(\sigma_{\mathrm{plateau}}^{\mathrm{d}} - \sigma_0^{\mathrm{d}}\right) \cdot \Delta t = 2\lambda l \rho_{\mathrm{c}} \cdot \Delta v, \tag{9}$$

where λl is the half length of the fold under impact loading, λ is the reduced fold length due to higher order buckling under impacting, $l = 0.821\sqrt[3]{hD^2}$ is the half-length of fold under quasi-static loading, and $\Delta v = V$ is the velocity variation of the cell wall involved in the fold during the time interval Δt. The time interval is dependent on the crushing velocity and fold length, given by

$$\Delta t = \frac{2l - 2\beta h}{V}, \tag{10}$$

where β represents the densified extent at the end of the folding. Finally, upon substituting Eqs. (7), (8), and (10) into Eq. (9), the dynamic plateau strength imparted on the impact side is obtained as

$$\sigma_{\mathrm{plateau}}^{\mathrm{d}} = 6.63\sigma_{\mathrm{ys}}\left(\frac{h}{D}\right)^{\frac{5}{3}}\left(1 + \frac{\rho_{\mathrm{s}} V c_{\mathrm{p}}}{\sigma_{\mathrm{ys}}}\right) + \frac{4}{\sqrt{3}} \cdot \frac{h/D}{1 - \beta h / \lambda l} \cdot \rho_{\mathrm{s}} V^2. \tag{11}$$

The fidelity of Eq. (11) is demonstrated by comparison with FE simulations, as shown in Fig. 8. The agreement is good by setting $\lambda = \beta = 1$, meaning that the fold length under impact loading equals that of the quasi-static value and the fold is completely densified. In addition, the normalized crushing plateau stress increases exponentially with the dimensionless parameter $\sqrt{\rho_{\mathrm{s}} V^2/\sigma_{\mathrm{ys}}}$, suggesting that inertia effect plays an important role.

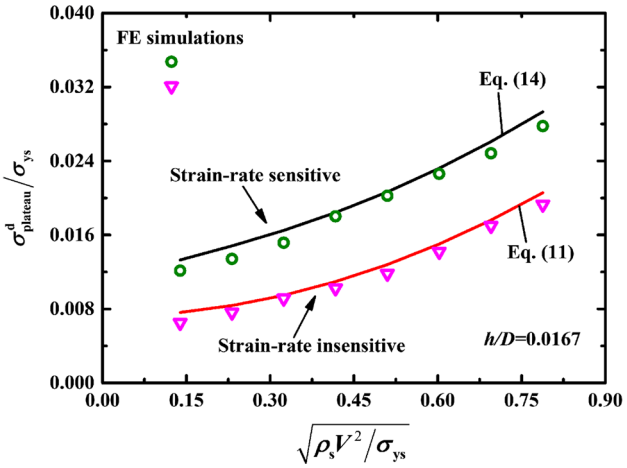

Fig. 8 Crushing plateau stress plotted as a function of dimensionless loading parameter $\sqrt{\rho_{\mathrm{s}} V^2/\sigma_{\mathrm{ys}}}$: comparison between analytical predictions and FE simulations

4 Effect of strain-rate sensitivity

For metallic honeycombs subjected to high-speed impact loading, it is important to quantify the effect of strain-rate sensitivity on dynamic crushing. We adopt the Cowper-Symonds model to characterize the strain-rate dependent behavior of the parent material, as described in Sect. 2. Figure 9 displays the numerically simulated temporal evolution of plastic strain distribution along cell wall height for both strain-rate sensitive and insensitive materials. The strain-rate sensitivity is seen to smear out plastic shocks over a finite width, thus diffusing the plastic front and rapidly increasing the wave speed. As a result, the duration of the peak stress plateau becomes much shorter, actually almost invisible (Fig. 3b), relative to that of strain-rate insensitive honeycombs (Fig. 3a). This explains why no obvious peak stress plateau had been observed in honeycombs subjected to impact loading by numerous existing studies [24, 27, 28]. Therefore, the analytical prediction of truncation strain ε_{t} by Eq. (6) is no longer applicable for strain-rate sensitive honeycombs.

The results of FE simulations presented in Figs. 3, 4 and 8 indicate that the most apparent influence of strain-rate sensitivity is the enhancement in both the peak stress and the crushing stress. Inspection of Figs. 6 and 8 reveals further that, as the impact velocity is increased, the increment in crushing stress due to strain-rate sensitivity increases slightly, while the increment in peak stress increases obviously. This indicates that the enhancing mechanisms of strain-rate sensitivity for dual-level plateau stresses are different, as illustrated below.

(1) *Peak stress*. To incorporate the strain-rate sensitivity, the static flow stress σ_{ys} is replaced by the dynamic flow

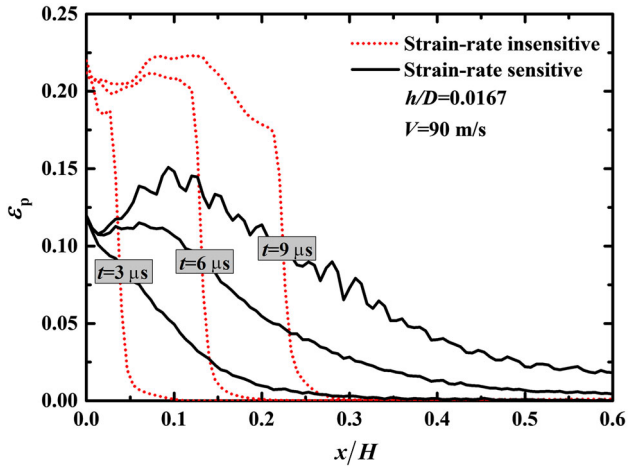

Fig. 9 Temporal variation in plastic strain distribution along Lagrange location of cell wall height

stress as expressed in Eq. (2). Correspondingly, for a strain-rate sensitive honeycomb, the theoretical prediction of its dynamic peak stress is given by

$$\sigma_{\text{peak}}^{\text{d}} = \sigma_{\text{ys}}\overline{\rho}\left[1+\left(\frac{\dot{\varepsilon}_1}{C}\right)^{1/P}\right] + \rho_{\text{c}} V c_{\text{p}}, \tag{12}$$

where $\dot{\varepsilon}_1$ is the local strain-rate in the plastic region

$$\dot{\varepsilon}_1 = \frac{V}{L_{\text{c}}}. \tag{13}$$

The strain-rate increases linearly with impact velocity, causing the peak stress to continuously increase as the impact velocity is increased. Comparisons between the theoretical predictions of Eq. (12) and the FE simulation results indicate that the theoretical predictions appear to underestimate the peak stress when the impact velocity is increased. The underestimation may be attributed to the underestimated plastic wave speed, since plastic wave speed should have increased as a result of strain-rate sensitivity.

(2) *Crushing stress*. For strain-rate sensitive honeycombs, the theoretical prediction of dynamic plateau stress can be expressed as:

$$\sigma_{\text{plateau}}^{\text{d}} = 6.63\sigma_{\text{ys}}\left(\frac{h}{D}\right)^{\frac{5}{3}}\left(1+\frac{\rho_{\text{s}} V c_{\text{p}}}{\sigma_{\text{ys}}}\right)\left[1+\left(\frac{\dot{\varepsilon}_2}{C}\right)^{1/P}\right] + \frac{4}{\sqrt{3}}\cdot\frac{h/D}{1-\beta h/\lambda l}\cdot\rho_{\text{s}} V^2, \tag{14}$$

where $\dot{\varepsilon}_2$ denotes the local strain-rate of cell wall rolling at plastic hinges, which has been well characterized [1, 24]. The average strain ε_2 during rolling equals $h/4b$, where $b = 0.683\sqrt[3]{h^2 D}$ is the rolling radius [1]. The local strain-rate can then be expressed as $\dot{\varepsilon}_2 = \frac{\varepsilon_2}{\lambda l/V}$. Comparisons between the theoretical predictions made by Eq. (14) and the FE simulations in Fig. 8 demonstrate the veracity of the theoretical model.

In summary, the difference in enhancing mechanisms of strain-rate sensitivity for dual-level plateau stresses is mainly attributed to the different forms of local strain rates. It should, nonetheless, be pointed out that the focus of the foregoing analysis has been placed upon quantifying the influence of strain-rate sensitivity on dual-level plateau stresses. Further investigations are needed to explore and understand the physical mechanisms underlying the reduction of truncation strain due to strain-rate sensitivity.

5 Concluding remarks

Dual-level stress plateaus occurring in metallic hexagonal honeycombs under high-speed out-of-plane impact loading have been quantified and the underlying mechanisms explored, using a combined numerical and analytical approach. The effect of strain-rate sensitivity is accounted for by introducing the Cowper–Symonds model for dynamic flow stress. The prediction is validated against existing test data, with good agreement achieved.

When the honeycomb is subjected to impact loading, bucklewaves are initiated and propagate in cell walls, followed by buckling and progressive folding of cell walls, which cause a relatively short peak stress plateau and subsequent prolonged crushing stress plateau. The abrupt stress drop from peak to crushing plateau can be explained in a way similar to quasi-static buckling of a clamped plate. For strain-rate insensitive honeycombs, the dynamic peak plateau stress, crushing plateau stress and truncation strain are all sensitive to cell wall aspect ratio and loading speed. For strain-rate sensitive honeycombs, the dual-level stresses are both elevated, whereas the duration of the peak stress plateau is shortened.

Acknowledgements This work was supported by the National Natural Science Foundation of China (Grants 11472209 and 11472208), the China Postdoctoral Science Foundation (Grant 2016M600782), the Postdoctoral Scientific Research Project of Shaanxi Province (Grant 2016BSHYDZZ18), the Zhejiang Provincial Natural Science Foundation of China (Grant LGG18A020001), the Fundamental Research Funds for Xi'an Jiaotong University (Grant xjj2015102), the Jiangsu Province Key Laboratory of High-end Structural Materials (Grant hsm1305), and the Natural Science Basic Research Plan in Shaanxi Province of China (Grant 2018JQ1078).

References

1. Wierzbicki, T.: Crushing analysis of metal honeycombs. Int. J. Impact Eng. **1**, 157–174 (1983)

2. Zhang, J., Ashby, M.F.: The out-of-plane properties of honeycombs. Int. J. Mech. Sci. **34**, 475–489 (1992)
3. Zhang, Q.C., Yang, X.H., Li, P., et al.: Bioinspired engineering of honeycomb structure—using nature to inspire human innovation. Prog. Mater. Sci. **74**, 332–400 (2015)
4. Côté, F., Deshpande, V.S., Fleck, N.A., et al.: The out-of-plane compressive behavior of metallic honeycombs. Mater. Sci. Eng., A **380**, 272–280 (2004)
5. Wilbert, A., Jang, W.Y., Kyriakides, S., et al.: Buckling and progressive crushing of laterally loaded honeycomb. Int. J. Solids Struct. **48**, 803–816 (2011)
6. Enboa, W., Jiang, W.S.: Axial crush of metallic honeycombs. Int. J. Impact Eng. **19**, 439–456 (1997)
7. Hu, L.L., He, X.L., Wu, G.P., et al.: Dynamic crushing of the circular-celled honeycombs under out-of-plane impact. Int. J. Impact Eng. **75**, 150–161 (2015)
8. Xu, S.Q., Beynon, J.H., Ruan, D., et al.: Experimental study of the out-of-plane dynamic compression of hexagonal honeycombs. Compos. Struct. **94**, 2326–2336 (2012)
9. Sun, D., Zhang, W., Wei, Y.: Mean out-of-plane dynamic plateau stresses of hexagonal honeycomb cores under impact loadings. Compos. Struct. **92**, 2609–2621 (2010)
10. Hou, X.H., Deng, Z.C., Zhang, K.: Dynamic crushing strength analysis of auxetic honeycombs. Acta Mech. Solida Sin. **29**, 490–501 (2016)
11. Calladine, C.R., English, R.W.: Strain-rate and inertia effects in the collapse of two types of energy-absorbing structure. Int. J. Mech. Sci. **26**, 689–701 (1984)
12. Harrigan, J.J., Reid, S.R., Peng, C.: Inertia effects in impact energy absorbing materials and structures. Int. J. Impact Eng. **22**, 955–979 (1999)
13. Ferri, E., Antinucci, E., He, M.Y., et al.: Dynamic buckling of impulsively loaded prismatic cores. J. Mech. Mater. Struct. **1**, 1345–1365 (2006)
14. Tilbrook, M.T., Radford, D.D., Deshpande, V.S., et al.: Dynamic crushing of sandwich panels with prismatic lattice cores. Int. J. Solids Struct. **44**, 6101–6123 (2007)
15. Radford, D.D., Mcshane, G.J., Deshpande, V.S., et al.: Dynamic compressive response of stainless-steel square honeycombs. ASME J. Appl. Mech. **74**, 658–667 (2007)
16. Ferri, E., Deshpande, V.S., Evans, A.G.: The dynamic strength of a representative double layer prismatic core: a combined experimental, numerical, and analytical assessment. ASME J. Appl. Mech. **77**, 061011 (2010)
17. Vaughn, D.G., Hutchinson, J.W.: Bucklewaves. Eur. J. Mech. A: Solids **25**, 1–12 (2005)
18. Vaughn, D.G., Canning, J.M., Hutchinson, J.W.: Coupled plastic wave propagation and column buckling. ASME J. Appl. Mech. **72**, 1–8 (2005)
19. Zhang, K., Deng, Z.C., Xu, X.J., et al.: Symplectic analysis for wave propagation of hierarchical honeycomb structures. Acta Mech. Solida Sin. **28**, 150–161 (2015)
20. Hooputra, H., Gese, H., Dell, H., et al.: A comprehensive failure model for crashworthiness simulation of aluminum extrusions. Int. J. Crashworthiness **9**, 449–464 (2004)
21. Cowper, G.R., Symonds, P.S.: Strain-hardening and strain-rate effects in the impact loading of cantilever beams. Division of Applied Mathematics Report No. 28, Brown University, Providence, RI, USA (1957)
22. Han, B., Qin, K.K., Yu, B., et al.: Honeycomb-corrugation hybrid as a novel sandwich core for significantly enhanced compressive performance. Mater. Des. **93**, 271–282 (2016)
23. Han, B., Wang, W.B., Zhang, Z.J., et al.: Performance enhancement of sandwich panels with honeycomb-corrugation hybrid core. Theor. Appl. Mech. Lett. **6**, 54–59 (2016)
24. Tao, Y., Chen, M., Pei, Y., et al.: Strain-rate effect on mechanical behavior of metallic honeycombs under out-of-plane dynamic compression. ASME J. Appl. Mech. **82**, 021007 (2015)
25. Reid, S.R., Peng, C.: Dynamic uniaxial crushing of wood. Int. J. Impact Eng. **19**, 531–570 (1997)
26. Karagiozova, D., Alves, M.: On the dynamic compression of cellular materials with local structural softening. Int. J. Impact Eng. **108**, 153–170 (2017)
27. Tao, Y., Chen, M., Pei, Y., et al.: Strain-rate effect on the out-of-plane dynamic compressive behavior of metallic honeycombs: experiment and theory. Compos. Struct. **132**, 644–651 (2015)
28. Hou, B., Zhao, H., Pattofatto, S., et al.: Inertia effects on the progressive crushing of aluminum honeycombs under impact loading. Int. J. Solids and Struct. **49**, 2754–2762 (2012)